



Published in final edited form as:

IEEE Trans Biomed Eng. 2008 January ; 55(1): 257–266. doi:10.1109/TBME.2007.900540.

A Novel Transcranial Magnetic Stimulator Inducing Near Rectangular Pulses with Controllable Pulse Width (cTMS)

Angel V. Peterchev [Member, IEEE],

The Division of Brain Stimulation and Therapeutic Modulation, Department of Psychiatry, Columbia University, New York, NY 10032, USA (ap2394@columbia.edu)

Reza Jalinous, and

Magstim Company US, LLC, Woburn, MA 01801, USA and also with the Division of Brain Stimulation and Therapeutic Modulation, Department of Psychiatry, Columbia University, New York, NY 10032, USA

Sarah H. Lisanby

The Division of Brain Stimulation and Therapeutic Modulation, Department of Psychiatry, Columbia University, New York, NY 10032, USA

Abstract

A novel transcranial magnetic stimulation (TMS) device with controllable pulse width (PW) and near rectangular pulse shape (cTMS) is described. The cTMS device uses an insulated gate bipolar transistor (IGBT) with appropriate snubbers to switch coil currents up to 7 kA, enabling PW control from 5 μ s to over 100 μ s. The near-rectangular induced electric field pulses use 22–34% less energy and generate 67–72% less coil heating compared to matched conventional cosine pulses. CTMS is used to stimulate rhesus monkey motor cortex *in vivo* with PWs of 20 to 100 μ s, demonstrating the expected decrease of threshold pulse amplitude with increasing PW. The technological solutions used in the cTMS prototype can expand functionality, and reduce power consumption and coil heating in TMS, enhancing its research and therapeutic applications.

Index Terms

Transcranial magnetic stimulation (TMS); biomagnetics; magnetic fields; electric fields; neuromuscular stimulation; pulse generation; pulse shaping circuits; pulse power systems; insulated gate bipolar transistors; pulse width (PW); energy measurement; heating; biomembranes; bioelectric potentials

I. Introduction

Transcranial magnetic stimulation (TMS) is a non-invasive tool for the study of the human brain that is being investigated as a potential therapeutic agent in psychiatry and neurology. A pulsed current sent through a coil produces a magnetic field that, in turn, induces electric field in the brain, which can cause neurons to fire. Available TMS devices induce damped

Copyright ©2007 IEEE

Correspondence to: Angel V. Peterchev.

This work was presented in part at the Annual Meeting of the American College of Neuropsychopharmacology (ACNP), Hollywood, Florida, USA, December 3–7, 2006 [1].

Personal use of this material is permitted. However, permission to use this material for any other purposes must be obtained from the IEEE by sending an email to pubs-permissions@ieee.org.

cosine electric field pulses. The pulse amplitude can be adjusted over a wide range, whereas control over the pulse width (PW) is non-existent or very limited. We have developed a novel TMS device which induces near rectangular electric field pulses with PW controllable over a wide range (cTMS).¹ Besides enabling PW adjustment, the near rectangular pulse shape reduces power consumption and coil heating. Thus, cTMS can expand the functionality and improve the efficiency of TMS as a clinical and research tool.

PW control of the TMS stimulus enables response characterization of different neuronal populations and optimization of the PW for various research and clinical applications. For example, the strength-duration curve relates the pulse amplitude or energy for threshold stimulation with the PW (Fig. 1) [2], [3]. The strength-duration curve of a neuronal population can be derived empirically by delivering TMS pulses with different PW while adjusting the amplitude to yield threshold stimulation. The strength-duration curve can be used to estimate neuronal membrane time constants [2]. This time constant depends on the biophysical properties of axonal membranes, which could vary as a function of age, gender, disease state, medication effects, treatment effects, and other factors. Thus, membrane time constant measurement can be a useful clinical and research tool that complements nerve conduction measurements [2], [4]. Further, membrane time constant measurements can inform neuronal modeling work which can contribute to understanding the mechanisms of TMS.

TMS with adjustable PW could also be used to study and selectively target distinct neuronal populations that overlap in space. For example, in peripheral nerves the motor threshold is lower than the sensory threshold for brief pulses, whereas it is higher than the sensory threshold for longer stimuli [3]. Similarly, it has been suggested that the ratio of cortical motor threshold to scalp sensory threshold is lower for brief pulses than for long stimuli [5]. Therefore, using briefer pulses could improve the tolerability of TMS by reducing unpleasant scalp sensations. Finally, within a cortical region, cTMS might be able to selectively activate distinct neuronal population possessing different strength-duration characteristics, thereby improving the effective spatial and functional resolution of TMS through selective targeting.

The effect of TMS PW on neuronal activation in the brain and the scalp has not been fully explored due to the relative difficulty in modifying PW in conventional TMS machines. Since the introduction of TMS in 1985 [6], the stimulator topology has remained largely unchanged. In conventional TMS devices, a capacitor is discharged through the stimulating coil inducing a damped cosine electric field pulse [7]. The circuit topology of a conventional monophasic TMS device is given in Fig. 2(a), with representative waveforms shown with dashed line in Fig. 3. Conventional TMS devices use a silicon controlled rectifier (SCR, a type of thyristor) to implement the discharge switch Q . The switching characteristic of SCRs does not allow them to be turned off at an arbitrary point in time. In particular, once an SCR is turned on by applying a current pulse to the gate terminal, it can be turned off only when the anode current reaches zero [8, Ch5]. Thus, the SCR switch can only initiate the pulse but cannot control its PW. In this case, the PW is determined by the resonant period of the capacitor C and the coil L . For all conventional TMS pulse types, the initial electric field phase lasts for $t_p = T/4$ seconds, where $T \approx 2\pi\sqrt{LC}$ is the circuit resonant period. Typically, t_p is in the range of 50 to 100 μ s. For a given coil, the only way to alter PW is to change the capacitance C . Most TMS devices have a fixed single capacitance value, precluding PW control. Some newer commercial stimulators offer a choice of two capacitor configurations resulting in two discrete PW settings [9]. However, besides the limitation of only two PW

¹cTMS technology is subject of patent application by Columbia University.

choices in these devices, the PW range is very restricted (1.0 : 1.4). Barker et al. modified a commercial monophasic stimulator to use a reconfigurable network of three capacitors allowing a choice of six magnetic field rise times [2]. Barker and colleagues used this device to measure the strength-duration curves of motor cortical and peripheral neurons. This approach still provides only discrete pulse-width adjustment, and requires powering down the system to manually insert connectors configuring the capacitors. Further, implementing this system with electronically controlled switches would be impractical since it would require the use of 7 high-power semiconductor devices and/or relays, with up to 3 switches connected in series in some capacitor configurations. Panizza et al. attempted to study the effect of different PWs by using a set of stimulating coils with different inductances, but failed to observe a significant effect [3]. They pointed out that enlarging the inductance increases the PW, but decreases the amplitude of the induced current. The amplitude reduction tends to cancel out the extended pulse duration, and consequently no effect of PW on neuronal activation was observed. Furthermore, the spatial profile of the magnetic field inevitably varies among coils, and the coils have to be repositioned over the target site, introducing spatial uncertainty.

Besides the limited control over the PW, in existing TMS devices the pulse is restricted to a damped cosine shape. The progressive discharge of the capacitor during the cosine pulse deteriorates the electrical efficiency since lower voltages are associated with inefficient energy transfer to the coil [10]. In contrast, rectangular pulses provide more efficient energy transfer to the coil, since the capacitor remains at near peak voltage throughout the pulse, resulting in reduced power dissipation and coil heating, as we demonstrate in Sec. IV-C. The use of rectangular pulses can substantially benefit high-frequency, high-power TMS applications such as in magnetic seizure therapy (MST), where excessive power consumption and coil heating are presently major limitations [11]. Finally, while the discussion above was illustrated for a monophasic TMS device, the same limitations on PW adjustment and cosine pulse shape apply to biphasic and polyphasic stimulators [7].

In this paper we present the circuit topology, implementation, and test results of a cTMS device which, in contrast to existing TMS machines, allows easy PW adjustment over a wide continuous range and produces near rectangular electric field pulses that improve the electrical efficiency and reduce coil heating.

II. Circuit Description

The basic circuit topology of the cTMS device is given in Fig. 2(b). It is similar to a conventional monophasic TMS stimulator [Fig. 2(a)] with the main difference that the switch Q is implemented with a semiconductor device such as an insulated gate bipolar transistor (IGBT) which, unlike an SCR, can be turned off from the gate terminal. Switch Q connects the stimulating coil L to the energy-storage capacitor C , causing the coil current to ramp up, which, in turn, induces electric field in the brain proportional to the coil current rate of change. By choosing when to turn off Q , the operator determines the electric field PW. The PW is limited to a quarter resonant period $\pi\sqrt{LC}/2$, which corresponds to complete discharge of C . For brief PWs ($t_p \ll \pi\sqrt{LC}/2$), the coil current rise is approximately linear and the induced electric field pulse is near rectangular [see Fig. 3(a–b)]. Thus, by choosing an appropriately large capacitance C , a wide range of PW control and near rectangular initial (positive) phase of the induced pulses can be effected. A further topological difference from conventional monophasic TMS devices is that the freewheeling diode D and the energy dissipation resistor R are connected across the coil L , rather than across the capacitor C , to provide a discharge path for the coil current when Q is turned off. Therefore, after Q is turned off the coil current decays exponentially, inducing a negative electric field. Through the device controller, the user specifies the voltage of capacitor C

which determines the amplitude of the induced electric field, and the on-time of switch Q which sets the PW of the positive phase of the induced pulse.

Mathematically, the initial positive phase of the cTMS coil current ($0 < t < t_p$) is an underdamped oscillatory response, and the subsequent negative phase ($t > t_p$) is an exponentially decaying response. The expression for coil current is shown in equation (1), where t_p is the PW of the positive phase of the pulse, r is the combined series resistance of the capacitor, inductor and switch, and

$$\omega = \sqrt{\frac{1}{LC} - \left(\frac{r}{2L}\right)^2} \quad (2)$$

$$\sigma = \frac{r}{2L}. \quad (3)$$

The induced electric field in the brain is proportional to the rate of change of the coil current. The electric field as a function of time is given in equation (4), where δ is a proportionality coefficient which depends on the number of turns and geometry of the coil, and the electric conductivity profile of the brain. In the limit of small parasitic resistance $r \rightarrow 0$ (required for high efficiency), and large capacitor or brief pulse $t_p \ll \pi\sqrt{LC}/2$, the positive phase of the pulse approaches a rectangle

$$E(t) = \begin{cases} \delta \frac{V_C}{L}, & 0 < t \leq t_p \\ -\delta \frac{V_C t_p R}{L^2} \exp\left[-\frac{(t-t_p)R}{L}\right], & t > t_p. \end{cases} \quad (5)$$

From equations (4) and (5) it can be seen that the amplitude and rate of decay of the negative electric field phase depend on the value of the dissipation resistor R . For representative parameter values ($C = 716 \mu\text{F}$, $L = 16 \mu\text{H}$, $R = 0.1 \Omega$, $r = 20 \text{ m}\Omega$, $\delta = 3.2 \times 10^{-6} \text{ (V/m)/(A/s)}$, $V_C = 1200 \text{ V}$, $t_p = 49 \mu\text{s}$) equations (1) and (4) are plotted with solid line in Figures 3(a) and (b), respectively. In Fig. 3(c), the estimated neuronal membrane potential V_m is plotted for membrane time constant of $\tau_m = 150 \mu\text{s}$ [2], [12]. Further, in Fig. 3 the corresponding waveforms of a conventional monophasic stimulator (Magstim 200) with the same coil and initial capacitor voltage are plotted for comparison. Note that, in this example, the neuronal membrane depolarization produced by the cTMS and conventional pulses is the same [Fig. 3(c)], while for cTMS both the peak coil current and the area under the coil current waveform are smaller [Fig. 3(a)].

III. Implementation

A. Component Selection

While the basic circuit topology of TMS devices is simple, the circuit implementation requires careful component selection, layout, thermal management, and transient suppression, due to the very high operating voltages and peak currents [7], [10], [13]. The key circuit specifications of cTMS are given in Table I. These values are within the range of commercial monophasic TMS devices, however the cTMS circuit presents additional implementation challenges due to the forced coil current commutation which enables PW control. A practical implementation of the cTMS topology from Fig. 2(b) is shown in Fig. 4, and is discussed below.

Switches—To enable PW control, the turn on and turn off of switch Q have to be controllable from its gate terminal. For the pulse parameters typical in TMS (peak voltage <

3 kV, peak current < 10 kA, peak switch on-time < 200 μ s), suitable switch choices are IGBTs [14], [15], gate-controlled thyristors (GTOs), and GTO-derived devices such as integrated gate-commutated thyristors (IGCTs) [16]. IGBTs are easiest to use due to their simple and fast (1–2 μ s) turn-off behavior. Therefore, Q was implemented with a 4500 V/600 A (dc rating) IGBT module (Powerex, Youngwood, PA). These modules can withstand brief pulsed currents of about 10 times their dc rating. The voltage rating was chosen to be safely above the peak IGBT collector-emitter voltage appearing during switching transients. The IGBT was switched with a high-voltage optically-isolated gate drive (Applied Power Systems, Hicksville, NY) with output impedance of 4 Ω providing turn-on and -off times of about a microsecond. A custom-made controller sent triggering pulses to the gate drive via an optic cable, with PW set by the user. Free-wheeling diode D_1 was implemented with two series-connected fast 1800 V (measured breakdown voltage)/105 A diodes (Semikron, Nuremberg, Germany).

Energy-storage capacitors—To allow PW control over a significant range and to produce close to rectangular induced current pulses, the cTMS energy-storage capacitors have to be larger than those in conventional stimulators. The maximum capacitor voltage should be chosen to allow suprathreshold stimulation of the targeted neuronal population at the shortest desired PW. The capacitance value should be chosen based on the upper limit of the desired PW range. However, using excessively large capacitance would require large physical dimension of the machine, and will pose safety risks due to the increased energy storage. Longer PWs are also associated with higher currents, mechanical stress, and heating in the stimulating coil. Thus, the targeted operating range of a cTMS device has to be checked against safety and technical limitations.

In the cTMS prototype in Fig. 4, the energy storage capacitor C_1 was implemented with six oil-filled high-voltage pulse capacitors (General Atomics, San Diego, CA) in parallel. Each capacitor had a nominal value of 120 μ F, and the total measured capacitance was 711 μ F. The capacitor bank was charged by a Magstim Booster Module Plus paired with a voltage controller from a Magstim Rapid device (Magstim, Whitland, UK). Safety of this implementation is addressed in Sec. III-B.

Stimulating Coil—The cTMS device can be used with most available TMS coils (typical inductance range 10–35 μ H). Whereas in conventional TMS devices the PW depends on the inductance of the specific coil used, in cTMS the PW is independently set by the controller. For all experimental results reported here, a Magstim 5.5 cm mean diameter, 15.8 μ H, air-core round coil was used.

Snubbers—In cTMS, the coil current is forced to commute between the energy-storage capacitor bank C and the free-wheeling diode D when the coil current is at its peak [refer to Figures 3 and 2(b)]. As a result of the forced coil current commutation, the cTMS topology presents a more challenging transient behavior than conventional TMS devices. Careful component selection and layout, as well as the use of snubber circuits is required to minimize and manage the transient energy. Stray inductance in capacitor bank C_1 , diode D_1 , resistor R_1 , and their wiring to switch Q , as well as the finite switching times of Q and D_1 can cause large voltage spikes and power loss during Q turn off, which can result in damage to the semiconductor components [8, Ch15], [17, Ch11]. Therefore, the wiring and component placement in the cTMS device were arranged so as to minimize the stray inductance. Still, stray inductance cannot be completely eliminated. For example, capacitor bank series inductance of 150 nH with 7 kA current stores magnetic energy sufficient to produce a 27 kV spike on an IGBT switch with 10 nF collector capacitance. Therefore, snubber components were installed in parallel with the energy-storage capacitor bank C_1 and the switch Q to handle the turn-off transient. Snubber capacitor C_2 is mounted as close as

possible to the collector terminal of Q to prevent the collector voltage from overshooting during turn off as a result of the parasitic inductance of capacitor bank C_1 and the connecting wires. Capacitor C_3 is mounted tightly between the collector and emitter terminals of Q to suppress high-frequency high-voltage spikes. Further, the snubber circuit consisting of D_2 , R_2 , and C_4 transiently absorbs the current flowing through the coil L when Q is turned off, supporting the current commutation to D_1 and R_1 . Capacitor C_4 is not connected directly between the emitter and collector of Q to avoid large current spikes occurring when Q is turned on. Diode D_2 consists of three series-connected fast-recovery 1200 V/60 A diodes (International Rectifier, El Segundo, CA). Snubber capacitors C_{2-4} utilize high-voltage, high-current polypropylene and paper film/foil capacitors. These capacitors have to be large enough to hold the peak switch voltage below its rated limit. On the other hand, too large capacitance would increase switching losses. Approaches for sizing of snubber components are discussed in the literature (see, e.g., [17, Ch11]).

B. Safety

Single-pulse TMS is considered to be a minimal risk procedure in appropriately screened normal subjects [18], [19]. Table II compares key parameters related to safety of two commercial monophasic stimulators to the cTMS device. The commercial configurations are the Magstim 200 and the Magstim BiStim which can combine the output of two Magstim 200 devices [7]. For the cTMS device, the extreme case when the full capacitor bank is discharged through the coil is considered. This case is not intended to occur during normal operation of the device, but can happen if switch Q fails to turn off due to a fault in the controller, gate drive, or the power IGBT itself. It can be seen in Table II that parameters related to safety, such as peak voltage, stored energy, induced current density, and induced charge density do not exceed the values encountered in the conventional configurations. The induced charge density, which is directly linked to tissue damage, is well below the recommended safety limit of $40 \mu\text{C}/\text{cm}^2$ per pulse for all devices [20]. Further, the only component of the cTMS system that comes in contact with the subject is a commercial TMS coil, which has been designed and tested by the manufacturer to provide appropriate high-voltage insulation, heat dissipation, and structural integrity [10]. Finally, the stimulator circuit is mounted in a grounded metal enclosure to ensure electrical safety of the operator and containment of debris in case of component failure. As with all TMS devices, extreme care should be exercised when electrically testing or servicing the cTMS device, due to the potential presence of lethal voltages and charges.

IV. Experimental Results

A. Output

The cTMS device was tested with capacitor voltages up to 1.65 kV and peak coil currents up to 7 kA. The PW range of the initial electric field phase t_p was 5 to 160 μs . The experimental measurements of key cTMS switching waveforms are given in Fig. 5. The voltage at the IGBT collector V_{C2} was measured with a high-voltage probe [Fig. 5(a)]. The coil current I_L was measured with a Rogowski current probe (0.4 Hz–16 MHz bandwidth) [Fig. 5(b)]. The induced electric field was characterized with a single-turn 5 cm diameter search coil placed 2 cm from the face of the TMS coil [Fig. 5(c)]. The search coil signal V_s was connected to a first-order low-pass filter with 150 μs time constant which outputs a scaled estimate V_f of the neuronal membrane potential waveform [Fig. 5(d)] [2], [12]. The initial capacitor voltage was 993 V. The waveforms associated with PW of 20, 40, 60, 80, 100, and 120 μs are overlaid for comparison. As expected, the positive phase of the induced pulse comprises a portion of a cosine wave, which is close to rectangular for brief PWs. The negative phase of the pulse is exponentially decaying. Finally, from the emulated neuronal membrane potential it can be seen that longer PWs produce more membrane depolarization.

B. Switching Transients

As expected, Q turn off causes a voltage spike and ringing at Q collector [Fig. 5(a)] due to the parasitic inductance of the energy-storage capacitor bank C_1 and its wiring (see Sec. III-A). This parasitic inductance was estimated to be approximately 150 nH. The amplitude of the spike is successfully limited by the snubber capacitors, and does not exceed 10% of the initial C_1 voltage. Overshoot and ringing of Q emitter during turn off is expected as well, due to parasitic inductances and the forward recovery of the freewheeling diode D_1 . This behavior can be observed in the search coil waveform [Fig. 5(c)]. Due to the snubbers, Q collector-emitter voltage never exceeds about twice the initial capacitor voltage, and is thus well below the 4,500 V rating of the IGBT.

C. Power Consumption and Coil Heating

The power consumption of a TMS device can be expressed as

$$P = \frac{f_{train} \Delta W_C}{\eta} \quad (6)$$

where f_{train} is the pulse train frequency, ΔW_C is the energy dissipated per pulse, and η is the capacitor charger efficiency. The energy per pulse can be measured by subtracting the energy on all n capacitors in the power circuit before and after the pulse

$$\Delta W_C = \frac{1}{2} \sum_{i=1}^n C_i V_{C_i}^2(t=0) - \frac{1}{2} \sum_{i=1}^n C_i V_{C_i}^2(t \gg t_p). \quad (7)$$

In expression (7), it is assumed that the capacitor charger is turned off or contributes a negligible amount of charge during the pulse. The stimulating coil temperature is proportional to square of the coil current integrated over the pulse duration, which is sometimes called the load integral [13]

$$T_{coil} \propto \int_0^{t_p} I_L^2 dt + \int_{t_p}^{t \gg t_p} I_L^2 dt. \quad (8)$$

The two integrals in (8) correspond to the coil heating contributions of the positive and negative phases of the electric field pulse, respectively [refer to Fig. 3(b)].

To compare the efficiency and coil heating of the near-rectangular cTMS electric field pulses to those of conventional stimulators, the cTMS device was reconfigured to produce damped cosine pulses. To accomplish this, the energy-storage capacitor bank was reduced, and Q was kept on until the coil current decayed to zero, resulting in induced pulses with damped cosine shape identical to that of conventional monophasic TMS devices [refer to Fig. 3(b)]. Four capacitor configurations (63, 121, 183, and 240 μ F) were tested in cosine pulse mode, to provide a range of pulse widths (see Table III). Note that the 183 μ F configuration closely approximates a commercial Magstim 200 device which has a nominal capacitance value of 185 μ F [7]. The stimulating coil electric field was sensed with a search coil and the neuronal membrane response was emulated with a filter as described in Sec. IV-A. For all four capacitor configurations the initial capacitor voltage V_{C0} , which is directly proportional to the pulse amplitude, was adjusted to obtain equal peak filter voltage ($V_f = 2.82$ V), corresponding to equal neuronal membrane depolarization. The energy per pulse for each configuration was calculated with equation (7) and given in Table III. Note that in the cosine-pulse configurations, the energy-storage capacitors are completely discharged, therefore the second summation term in (7) is always zero. Further, the energy dissipated in

snubber capacitors C_3 and C_4 is not factored in the calculation of ΔW_C since these capacitors are not necessary in the conventional monophasic TMS configuration. Finally, the level of coil heating was estimated by calculating the first integral in (8) which is associated with the positive (depolarizing) phase of the electric field pulse. The load integral values are listed in Table III. The contribution of the negative pulse phase is not included since it depends on the value of the dissipation resistor R , which can be chosen arbitrarily.

After completing the measurements of the cosine-pulse TMS configurations, the full cTMS capacitor bank was reconnected. The initial capacitor voltage V_{C0} was set to each of the values used in the cosine-pulse configurations, and in each case the PW was adjusted so that the peak filter voltage equaled that with the cosine pulses ($V_f = 2.82$ V). The energy dissipation was calculated with (7), including the energy loss in snubber capacitors C_3 and C_4 , since the snubbers are essential for proper operation of the cTMS device. As with the cosine pulses, the coil heating was quantified with the load integral over the positive pulse phase in (8). The energy per pulse and the load integral for the cTMS configurations are given in Table III as well.

Based on the results in Table III, Fig. 6 provides a comparison of the power dissipation and coil heating for the cosine-pulse and cTMS devices. For clarity, the plots are normalized to the values for the Magstim 200 configuration. It should again be emphasized that all data points correspond to TMS configurations that yield the same amount of depolarization in a first-order low-pass filter model of the neuronal membrane, and therefore are expected to have the same physiological effect [2], [12]. For the conventional cosine pulses, the energy dissipation increases for lower capacitor voltages which correspond to larger capacitance values and longer PWs (see also Table III). These results are consistent with previous studies [2]. For cTMS, the dissipated energy and coil heating are lower than those for cosine pulses with the same initial capacitor voltage by 22–34% and 67–72%, respectively. For example, for the same capacitor voltage, and hence the same pulse amplitude, the near-rectangular cTMS pulse uses 30% less energy and contributes 71% less heat to the coil than the Magstim 200 damped cosine pulse.

It should be noted that the charger was not disconnected during the pulse measurements since it contributed charge of less than 0.1% of the initial C charge during the positive pulse phase, therefore not significantly affecting the energy measurement. Finally, the capacitor charger efficiency η is not included in the power consumption estimate for either configuration. However, it is reasonable to expect that a properly designed charger supplying a more narrow output voltage range close to the peak voltage, as is the case in cTMS, will have better efficiency than that of a conventional monophasic TMS device where the capacitor is charged up from zero after every pulse.

D. In Vivo Cortical Stimulation

To demonstrate the ability of cTMS to produce cortical stimulation *in vivo*, the motor threshold (MT) of rhesus monkeys was measured with cTMS for various PW setting. This study was approved by the Institutional Animal Care and Use Committees of New York State Psychiatric Institute and Columbia University. Five male rhesus monkeys [Macaca mulatta, age 9.4 ± 2.9 yr, weight 10.7 ± 2.7 kg (mean \pm standard deviation)] were sedated pre-intervention with ketamine 5.0 mg/kg and xylazine 0.3 mg/kg i.m., followed with ketamine 2.5 mg/kg boluses q45 min as needed to maintain sedation during the procedure. Physiological monitoring included ECG, pulse oximetry, end-tidal P_{CO_2} , and blood pressure. The TMS coil was placed at vertex with the initial pulse phase inducing clockwise current in the brain. Electromyography was measured with needle electrodes from the left first dorsal interosseous muscle. The MT, defined as the minimum pulse amplitude yielding at least 5 of 10 motor evoked potentials with peak-to-peak amplitude $> 50 \mu\text{V}$, was measured at five

PWs ($t_p = 20, 40, 60, 80,$ and $100 \mu\text{s}$) presented in pseudorandom order. All procedures were well tolerated with no adverse events from stimulation and no change in vital signs. The pulse amplitude corresponding to MT for the five subjects is plotted versus PW in Fig. 7. As expected, MT increases as PW decreases (refer to Fig. 1). These data were used in [1] to estimate the neuronal membrane time constant to be $116 \pm 25 \mu\text{s}$, which is close to that measured in awake humans, $152 \pm 26 \mu\text{s}$ [2].

V. Discussion

The cTMS prototype successfully demonstrated PW control by forced commutation of currents up to 7 kA between the IGBT and the free-wheeling diode. With appropriate snubber design, component selection, circuit layout, and wiring, the voltage transients associated with the IGBT turn off did not exceed the ratings of the power-train components. The design could be further optimized to reduce the turn-off voltage overshoots and ringing, while keeping the snubber capacitors in parallel with the IGBT, and hence the switching losses, reasonably small.

For the near rectangular cTMS pulse, the power consumption and coil heating are reduced by 22–34% and 67–72%, respectively, compared to matched conventional cosine pulses (see Sec. IV-C). The reason for this substantial performance improvement is that the progressive discharge of the capacitor during the cosine pulse deteriorates the electrical efficiency since lower voltages are associated with inefficient energy transfer to the coil [10]. In contrast, rectangular pulses provide more efficient energy transfer to the coil, since the capacitor remains at near peak voltage throughout the pulse. Consequently, the cTMS electric field remains at near-peak value during the positive pulse phase (see Fig. 3). The steady electric field strength depolarizes the neuronal membrane faster, resulting in briefer PW and lower peak coil current. Further, the cTMS coil current starts to decrease immediately after the neuronal membrane potential has reached its peak. The totality of these factors results in reduced power dissipation and coil heating in cTMS. One limitation of the efficiency measurements in Sec. IV-C is that, to match the neuronal depolarization effect of the rectangular and cosine waveforms, a simple first-order model of the neuronal membrane response was used. While it has been shown that a first-order model fits *in vivo* data well [2], there may be effects of the pulse shape that are not accounted for by the simplified model. Thus, future studies should compare the efficiency of the two pulse shapes using *in vivo* response matching. Further, the coil heating was estimated from the load integral of the coil current. A direct measurement using temperature sensors should be implemented in the future.

In the presented cTMS circuit topology, the energy returning from the stimulating coil is dissipated in resistor R , which results in low electrical efficiency for pulse trains, especially at high frequencies. The cTMS topology can be modified to deposit the coil energy on a capacitor and recycle it during the subsequent pulse, thus reducing power dissipation and allowing repetitive TMS operation at higher frequencies, analogously to conventional rapid-rate biphasic TMS devices. High-frequency, high-power TMS applications such as in magnetic seizure therapy (MST) [11] could particularly benefit from the reduced power consumption and coil heating of a rapid-rate, rectangular-pulse cTMS device. Furthermore, repetitive TMS with monophasic pulses may have a stronger and more selective neuromodulatory impact than conventional biphasic TMS, as suggested by recent studies [21]–[25]. Optimizing the tradeoff between transient voltage spikes and switching losses in the power train would be particularly relevant to rapid-rate cTMS devices.

VI. Conclusion

We have successfully developed the first TMS device capable of inducing near rectangular pulses with PW adjustable from 5 to over 100 microseconds. Coil currents up to 7 kA were force-commutated by an IGBT switch with appropriate snubbers, while the resulting transient voltage spikes did not exceed power-train component ratings. The key safety parameters of the cTMS device are within the range of existing commercial products. The rectangular pulses use 22–34% less electrical energy and contribute 67–72% less coil heating compared to a matched conventional cosine pulses. Suprathreshold stimulation of the rhesus monkey motor cortex was demonstrated with PWs as brief as 20 microseconds, and the expected inverse relationship between the PW and the threshold pulse amplitude was observed. Thus, state-of-the-art power electronics technology can enhance the functionality and efficiency of TMS, potentially extending its research and therapeutic applications.

Acknowledgments

This work was supported in part by a Faculty Development Award (Dr. Lisanby) by the New York State Office of Science, Technology and Academic Research. Dr. Lisanby has also received research support from the Magstim Company, Neuronics Inc., and Cyberonics Inc. (these companies did not provide support for the work presented here). The authors would like to thank Professors Seth R. Sanders and Anthony T. Barker for helpful discussions of the hardware implementation and safety, Timothy J. Spellman for assisting in the animal procedures, and Semikron GmbH for providing a free sample of the power diode module.

Biographies



Angel V. Peterchev (S'96–M'05) received the A.B. degree in physics and engineering sciences from Harvard University, Cambridge, MA, in 1999, and the M.S. and Ph.D. degrees in electrical engineering from the University of California, Berkeley, in 2002 and 2005, respectively.

Dr. Peterchev is presently Postdoctoral Research Scientist at the Division of Brain Stimulation and Therapeutic Modulation, Department of Psychiatry, Columbia University. In the summer of 2003, Dr. Peterchev was Co-op at the Portable Power Systems Group, National Semiconductor Corp., Santa Clara, CA. From 1997 to 1999, he was Member of the Rowland Institute at Harvard, where he developed scientific instrumentation. Dr. Peterchev's current research is focused on the development of technology and application paradigms for brain stimulation. His interests include pulsed power circuits and coil design for transcranial magnetic stimulation (TMS), simultaneous delivery of TMS with functional magnetic resonance imaging (fMRI) and electroencephalography (EEG), brain dynamics, and neural circuit modeling. He has also made contributions to analog and digital control of power converters, with applications to microprocessor voltage regulators and portable electronics.

Dr. Peterchev received the 1999 Tau Beta Pi Prize from Harvard University and a 2001 Outstanding Student Designer Award from Analog Devices, Inc.



Reza Jalinous received the B.Eng. degree in electronic computing and the Ph.D. degree in medical physics from University of Sheffield, England, UK, in 1982 and 1988, respectively.

Since 1998, Dr. Jalinous is Chief Executive Officer and Technical Director of Magstim Company US, LLC. Since 2007 he is also Adjunct Assistant Professor of Neuroscience at Columbia University. Dr. Jalinous is Founding Partner, and served as Technical and Clinical Director of Magstim Company Ltd, Wales, UK, during 1990–1998. From 1986 to 1990, he was Product Manager, Novamatrix Medical Systems, Inc., Wallingford, CT. Dr. Jalinous works on the development of transcranial magnetic stimulation (TMS) devices. He was part of the research team that is credited with accomplishing the first magnetically induced activation of the human cortex in 1985. Since then, Dr. Jalinous has introduced a number of innovations in TMS technology, leading to the first repetitive stimulator capable of high frequencies, air-cooled coils, and the first magnetic seizure therapy (MST) device. He is the chief designer of the Magstim line of commercial TMS devices.

Dr. Jalinous was co-recipient of the 1987 IEE/IMechE/Design Council Prize for Innovation (UK) for the development of clinical magnetic nerve stimulation.



Sarah H. Lisanby received the B.S. degree in mathematics and psychology in 1987 and the M.D. degree in 1991 from Duke University, Durham, NC. She completed residency in psychiatry at Duke University Medical Center.

Dr. Lisanby is presently Associate Professor of Clinical Psychiatry at Columbia University. In addition, she is Director of the Division of Brain Stimulation and Therapeutic Modulation at the New York State Psychiatric Institute, head of the Transcranial Magnetic Stimulation (TMS) Unit in the fMRI Research Center at Columbia, and the New York Presbyterian Hospital Brain Stimulation Service. She is also Director of the Brain Behavior Clinic at NYSPI. Dr. Lisanby has authored or coauthored over 150 articles, abstracts, chapters, books, reviews and editorials concerning TMS, electroconvulsive therapy (ECT), depression, and related topics. Her research team pioneered magnetic seizure therapy (MST) as a potential alternative treatment to ECT for major depression. Dr. Lisanby's group uses TMS in a variety of studies of normal and diseased brain function. She supervises clinical trials of TMS as a therapeutic tool in depression, schizophrenia, and other neuropsychiatric and neurological disorders. Dr. Lisanby conducts research with other forms of brain stimulation as well, such as transcranial direct current stimulation (tDCS) and vagus nerve stimulation (VNS).

Dr. Lisanby is the recipient of over 35 honors and awards, including the Gerald L. Klerman Award by the National Alliance for Research in Schizophrenia and Depression, and the 2004 Max Hamilton Memorial Prize of the Collegium Internationale Neuro-Psychopharmacologicum. She is also a member of the 2006–2008 Defense Sciences Study Group supported by DARPA and the Institute for Defense Analysis. Dr. Lisanby is the immediate Past President of the Association for Convulsive Therapy and the current Chairperson of the American Psychiatric Association Committee on ECT and Related Electromagnetic Therapies. She is also President of the International Society for Transcranial Stimulation and Member of the American College of Neuropsychopharmacology, among others.

References

1. Peterchev AV, Spellman TJ, Lisanby SH. cTMS: A novel TMS device inducing near rectangular pulses with controllable pulse width. *Neuropsychopharmacology*. 2006; 31(S1):S130.
2. Barker AT, Garnham CW, Freeston IL. Magnetic nerve stimulation: the effect of waveform on efficiency, determination of neural membrane time constants and the measurement of stimulator output. *Electroencephalogr Clin Neurophysiol Suppl*. 1991; 43:227–37. [PubMed: 1773760]
3. Panizza M, Nilsson J, Roth BJ, Basser PJ, Hallett M. Relevance of stimulus duration for activation of motor and sensory fibers: implications for the study of h-reflexes and magnetic stimulation. *Electroencephalogr Clin Neurophysiol*. 1992; 85(1):22–9. [PubMed: 1371740]
4. Rossini, PM.; Pauri, F. Central conduction time studies. In: Pascual-Leone, A.; Davey, NJ.; Rothwell, J.; Wassermann, EM.; Puri, BK., editors. *Handbook of Transcranial Magnetic Stimulation*. London: Arnold; 2002. p. 90-96.
5. Geddes LA. Optimal stimulus duration for extracranial cortical stimulation. *Neurosurgery*. 1987; 20(1):94–9. [PubMed: 3808283]
6. Barker AT, Jalinous R, Freeston IL. Non-invasive magnetic stimulation of human motor cortex. *Lancet*. 1985; 1(8437):1106–7. [PubMed: 2860322]
7. Jalinous, R. Principles of magnetic stimulator design. In: Pascual-Leone, A.; Davey, NJ.; Rothwell, J.; Wassermann, EM.; Puri, BK., editors. *Handbook of Transcranial Magnetic Stimulation*. London: Arnold; 2002. p. 30-38.
8. Kassakian, JG.; Schlecht, MF.; Verghese, GC. *Principles of Power Electronics*. Reading, MA: Addison-Wesley; 1991.
9. Medtronic A/S. MagPro X100 user guide including MagOption. 2003
10. Jalinous R. Technical and practical aspects of magnetic nerve stimulation. *J Clin Neurophysiol*. 1991; 8(1):10–25. [PubMed: 2019644]
11. Morales OG, Sackeim HA, Berman RM, Lisanby SH. Magnetic seizure therapy: development of a novel intervention for treatment resistant depression. *Clin Neurosci Res*. 2004; 4:59–70.
12. Corthout E, Barker AT, Cowey A. Transcranial magnetic stimulation: Which part of the current waveform causes the stimulation? *Exp Brain Res*. 2001; 141(1):128–32. [PubMed: 11685417]
13. Ruohonen, J.; Ilmoniemi, RJ. Basic physics and design of transcranial magnetic stimulation devices and coils. In: Hallett, M.; Chokroverty, S., editors. *Magnetic stimulation in clinical neurophysiology*. 2. Philadelphia, PA: Elsevier Butterworth-Heinemann; 2005. p. 17-30.
14. ABB Ltd. Insulated Gate Bipolar Transistor (igbt) Modules. 2006. [Online]. Available: <http://www.abb.com/>
15. Powerex Inc. Insulated Gate Bipolar Transistor (igbt) Modules. 2006. [Online]. Available: <http://www.pwr.com/>
16. ABB Ltd.. Integrated Gate-Commutated Thyristor (igct) Modules. 2006. [Online]. Available: <http://www.abb.com/>
17. Pressman, AI. *Switching Power Supply Design*. 2. New York: McGraw-Hill; 1998.
18. Wassermann EM. Risk and safety of repetitive transcranial magnetic stimulation: report and suggested guidelines from the international workshop on the safety of repetitive transcranial

- magnetic stimulation, June 5–7, 1996. *Electroencephalogr Clin Neurophysiol.* 1998; 108(1):1–16. [PubMed: 9474057]
19. Wassermann, EM. Safety and side-effects of transcranial magnetic stimulation and repetitive transcranial magnetic stimulation. In: Pascual-Leone, A.; Davey, NJ.; Rothwell, J.; Wassermann, EM.; Puri, BK., editors. *Handbook of Transcranial Magnetic Stimulation.* London: Arnold; 2002. p. 39–49.
 20. Agnew WF, McCreery DB. Considerations for safety in the use of extracranial stimulation for motor evoked potentials. *Neurosurgery.* 1987; 20(1):143–7. [PubMed: 3808255]
 21. Sommer M, Lang N, Tergau F, Paulus W. Neuronal tissue polarization induced by repetitive transcranial magnetic stimulation? *Neuroreport.* 2002; 13(6):809–11. [PubMed: 11997692]
 22. Antal A, Kincses TZ, Nitsche MA, Bartfai O, Demmer I, Sommer M, Paulus W. Pulse configuration-dependent effects of repetitive transcranial magnetic stimulation on visual perception. *Neuroreport.* 2002; 13(17):2229–33. [PubMed: 12488802]
 23. Tings T, Lang N, Tergau F, Paulus W, Sommer M. Orientation-specific fast rTMS maximizes corticospinal inhibition and facilitation. *Exp Brain Res.* 2005; 164(3):323–33. [PubMed: 15868175]
 24. Arai N, Okabe S, Furubayashi T, Terao Y, Yuasa K, Ugawa Y. Comparison between short train, monophasic and biphasic repetitive transcranial magnetic stimulation (rTMS) of the human motor cortex. *Clin Neurophysiol.* 2005; 116(3):605–13. [PubMed: 15721074]
 25. Taylor JL, Loo CK. Stimulus waveform influences the efficacy of repetitive transcranial magnetic stimulation. *J Affect Disord.* 2007; 97:271–276. [PubMed: 16887197]

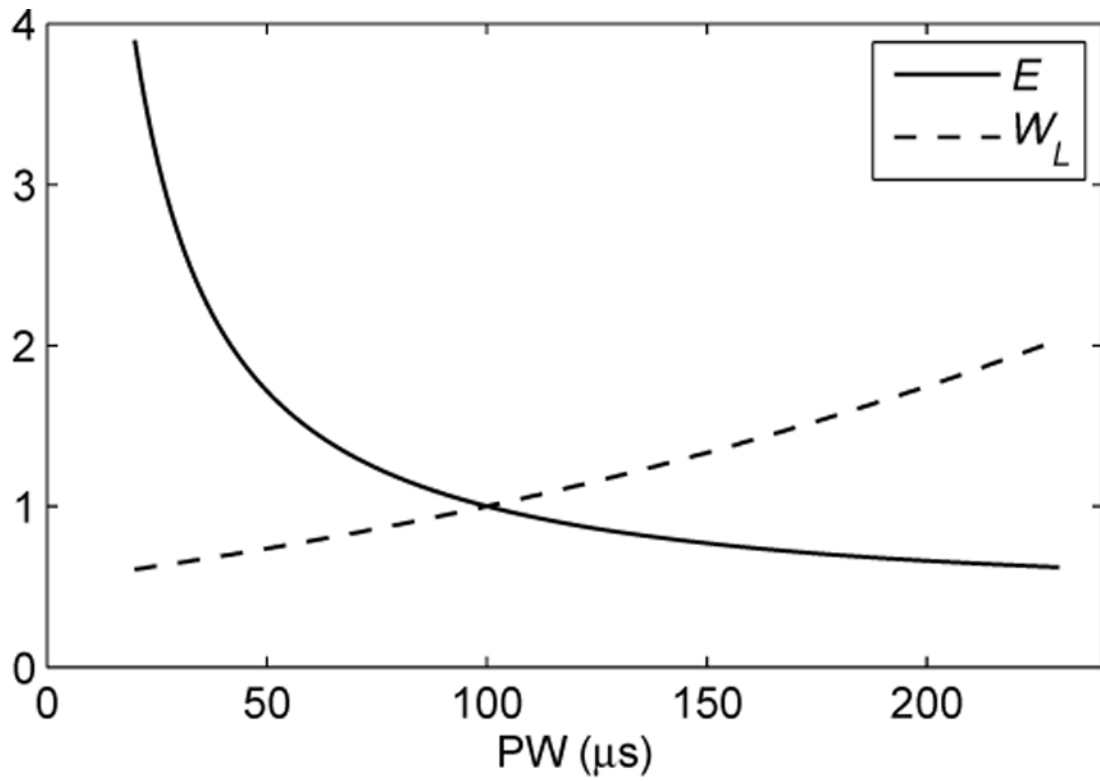


Fig. 1. Strength-duration curves linking rectangular pulse width (PW) to electric field strength E and coil energy W_L for threshold stimulation of neuron with membrane time constant of $\tau_m = 150 \mu s$. Curves are normalized to one at $PW = 100 \mu s$.

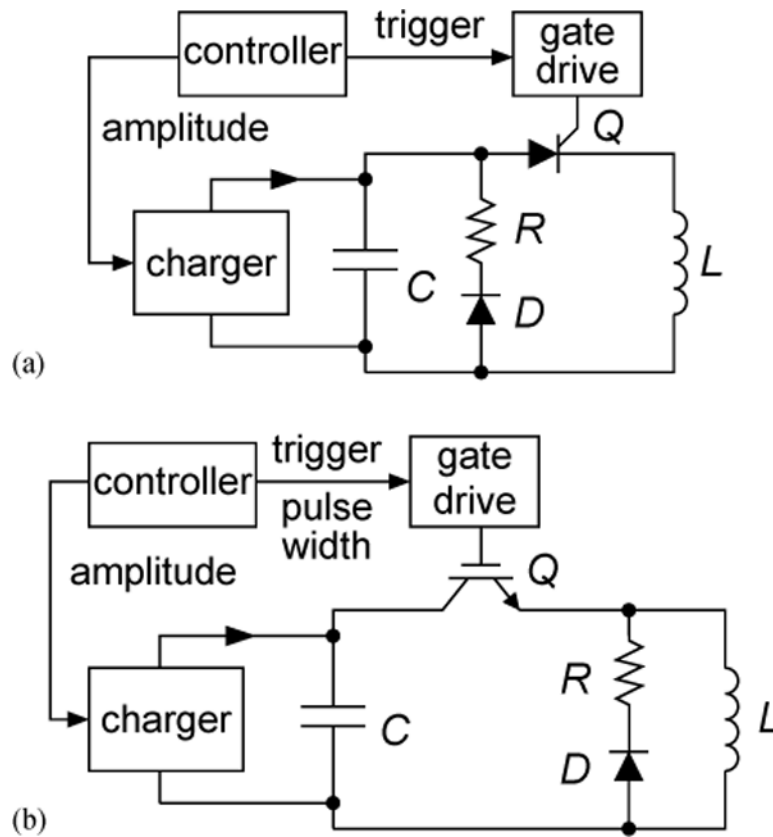


Fig. 2. Circuit topology of (a) conventional monophasic TMS device; (b) cTMS device which induces near rectangular electric field pulses with controllable PW.

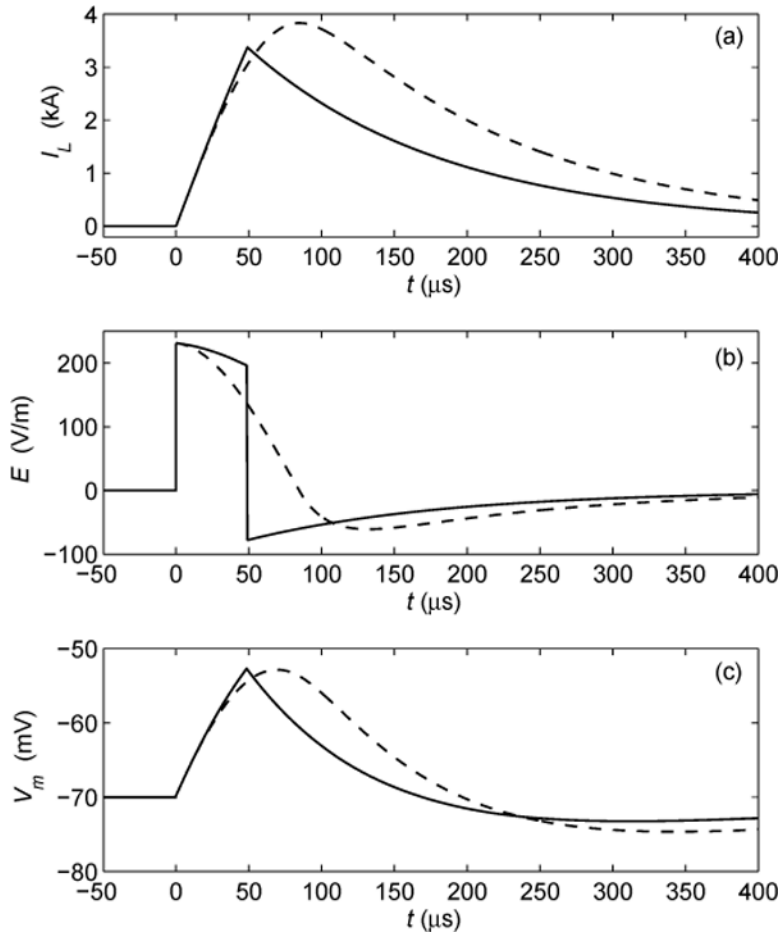


Fig. 3.

Comparison of simulated waveforms of conventional monophasic cosine TMS (dashed line) and cTMS (solid line). (a) Coil current I_L ; (b) induced electric field E (c) neuronal membrane potential V_m for membrane time constant of $150 \mu\text{s}$. In conventional TMS stimulators only pulse amplitude can be adjusted, while in cTMS device both pulse amplitude and width can be controlled. Near rectangular cTMS pulse shape results in less power consumption and coil heating.

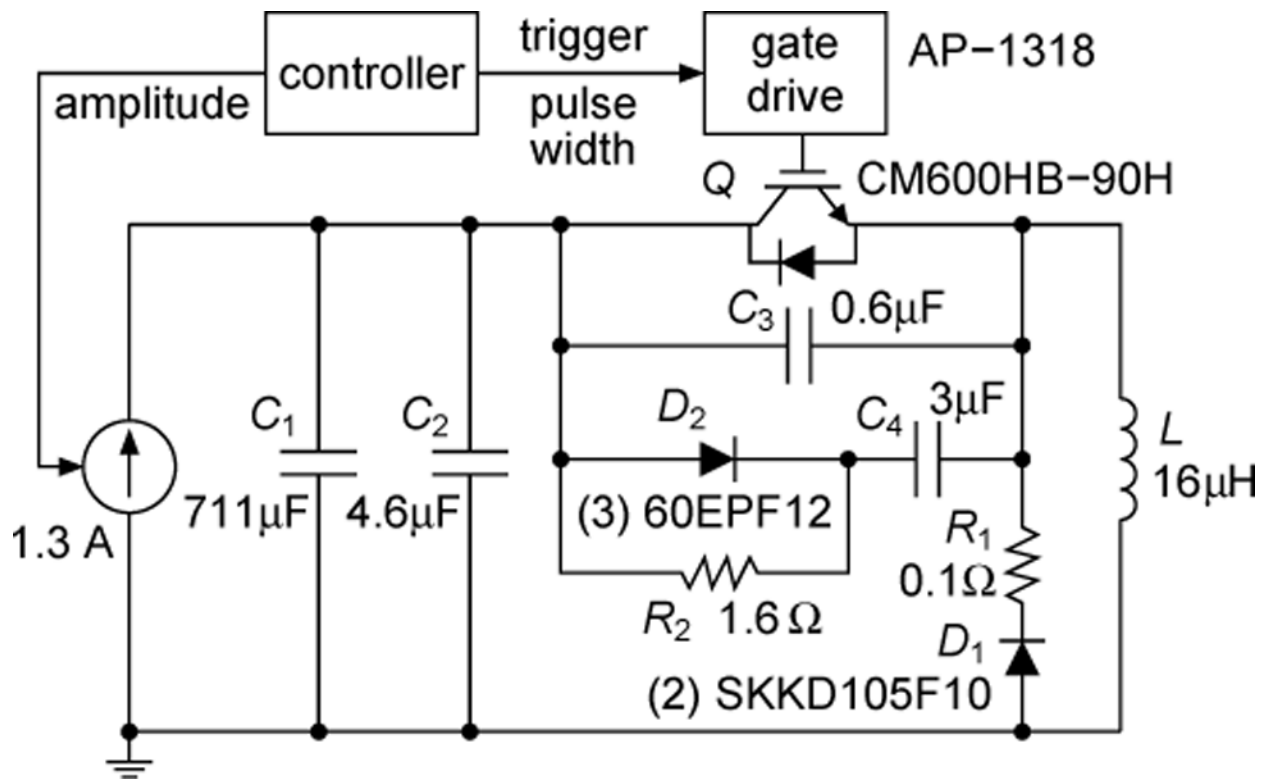


Fig. 4. Implementation schematic of cTMS device. Snubber circuits in parallel with capacitor bank C_1 and switch Q suppress voltage spikes associated with Q turn off and reduce power dissipation in Q .

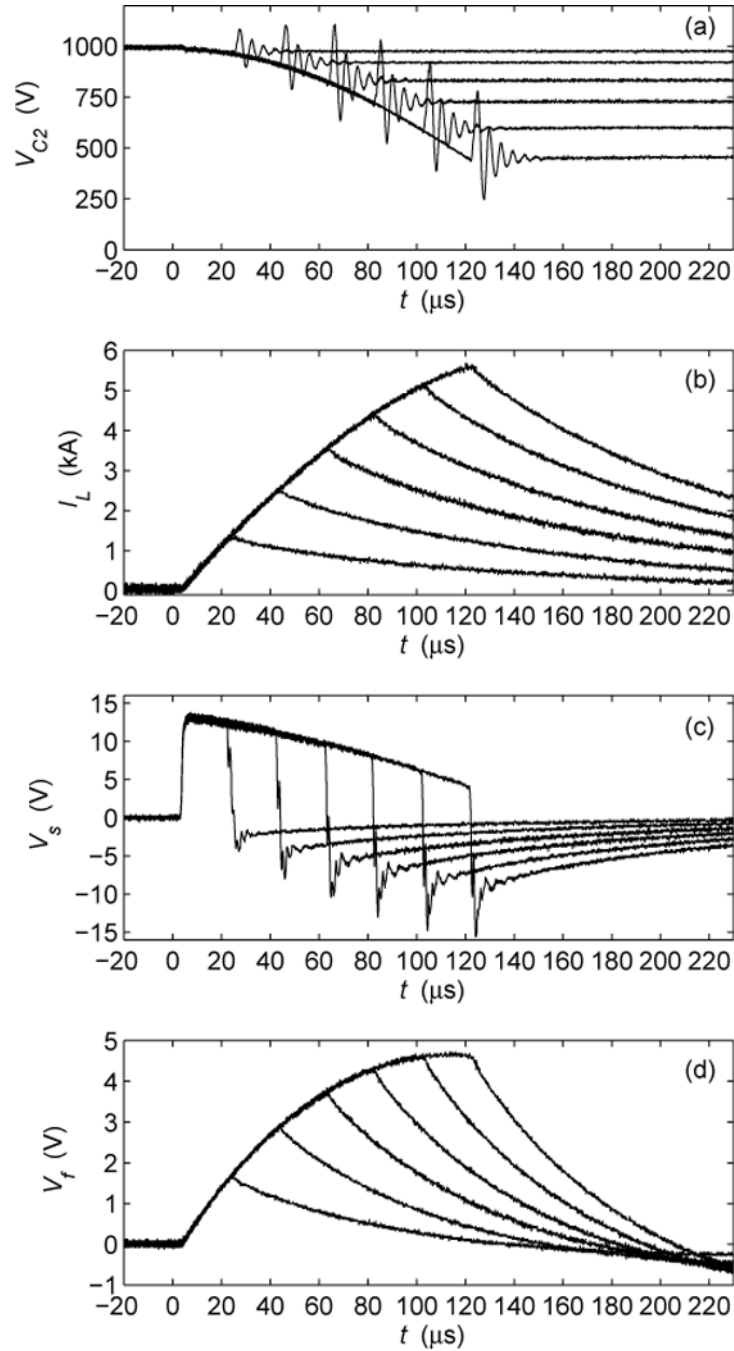


Fig. 5.

Measured cTMS waveforms for PWs of $t_p = 20, 40, 60, 80, 100,$ and $120 \mu\text{s}$: (a) IGBT collector voltage V_{C2} ; (b) coil current I_L ; (c) search coil voltage V_s proportional to induced electric field by TMS coil; (d) low-pass filtered search coil voltage V_f proportional to neuronal membrane potential for membrane time constant of $150 \mu\text{s}$.

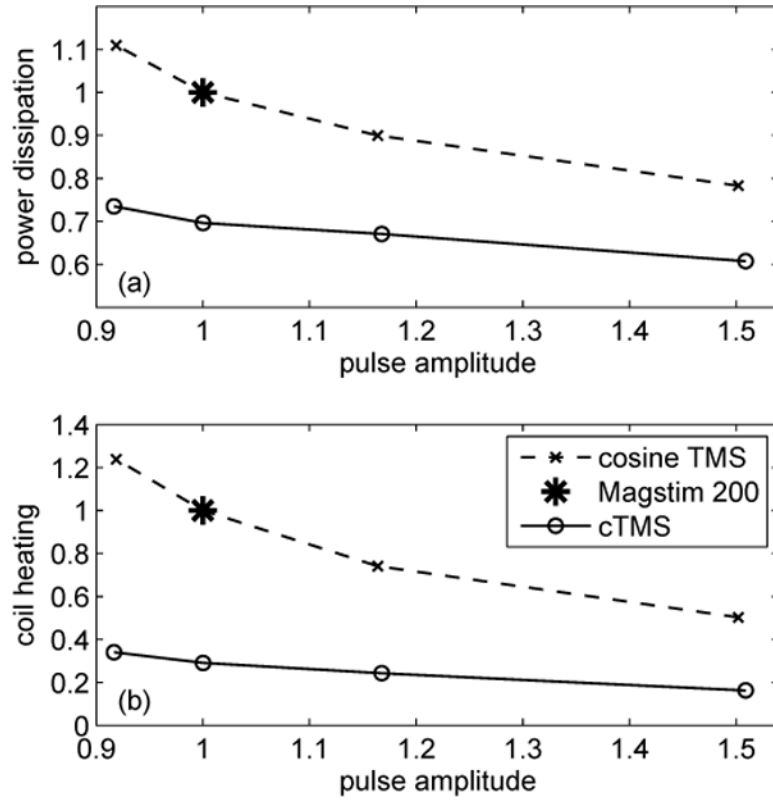


Fig. 6. Comparison of (a) power dissipation and (b) coil heating of conventional monophasic cosine TMS and cTMS, based on data from Table III. All values are normalized to those for Magstim 200. Pulse amplitude is directly proportional to initial capacitor voltage V_{C0} . Power dissipation is directly proportional to energy used per pulse ΔW_C . Coil heating is directly proportional to load integral $\int_0^p I_L^2 dt$. Note that all data points correspond to TMS configurations that yield same amount of neuronal depolarization, and therefore pulses with larger amplitude have briefer PW (refer to Table III).

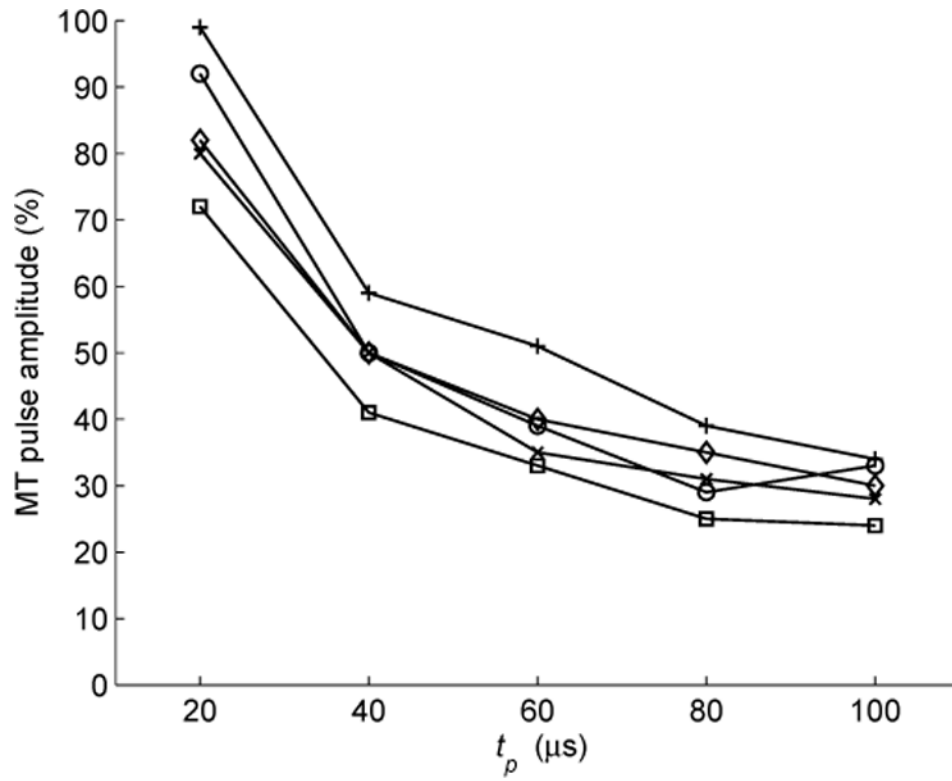


Fig. 7. CTMS pulse amplitude corresponding to cortical motor threshold (MT), given as percentage of maximum pulse amplitude for this device, versus PW t_p in 5 rhesus monkeys.

$$I_L(t) = \begin{cases} \frac{V_{C0}}{\omega L} \sin(\omega t) \exp(-\sigma t), & 0 < t \leq t_p \\ \frac{V_{C0} \sin \omega t_p}{\omega L} \exp \left[-\frac{(t - t_p)(R + r)}{L} - \sigma t_p \right], & t > t_p \end{cases}$$

(1).

$$E(t) = \begin{cases} \delta \frac{V_{C0}}{L} \left(\cos \omega t - \frac{\sigma}{\omega} \sin \omega t \right) \exp(-\sigma t), & 0 < t \leq t_p \\ -\delta \frac{V_{C0}(R+r) \sin \omega t_p}{\omega L^2} \exp \left[-\frac{(t-t_p)(R+r)}{L} - \sigma t_p \right], & t > t_p \end{cases}$$

(4).

TABLE I

CTMS SPECIFICATIONS

parameter		peak value	unit
V_C	capacitor voltage	1.65	kV
I_L	coil current	6	kA
$t_{p,eff}$	effective pulse width [†]	110	μ s
f_{train}	pulse train frequency	1	Hz

[†] time interval from zero to peak neuronal membrane depolarization, assuming membrane time constant $\tau_m = 150 \mu$ s

TABLE II

Monophasic stimulator peak parameter comparison[†]

parameter	stimulator type			unit
	Magstim 200	BiStim	cTMS	
V_C	2.8	2.8	1.65	kV
C	185	370	716	μF
W_C	725	1,450	981	J
I_c	8.7	12.0	9.5	kA
B	1.6	2.8	2.2	T
t_r	84	117	160	μs
E	540	540	319	V/m
J	19	19	11	mA/cm^2
ρ_q	1.0	1.3	1.0	$\mu\text{C}/\text{cm}^2$
ΔV_m	39	49	34	mV

[†]Peak values induced in brain tissue (grey matter conductivity = 0.35 S/m) with 70 mm Magstim figure-of-eight coil. Neuronal membrane time constant $\tau_M = 150 \mu\text{s}$.

TABLE III

Monophasic stimulator efficiency comparison[‡]

V_{C_0} (V)	conventional cosine TMS				cTMS ($C = 716 \mu\text{F}$)			
	C^{\ddagger} (μF)	t_p (μs)	ΔW_C (J)	$\int_0^P I_L^2 dt (\text{A}^2 \text{s})$	t_p (μs)	ΔW_C (J)	$\int_0^P I_L^2 dt (\text{A}^2 \text{s})$	
1,327	63	49	56	165	28	43	54	
1,028	121	66	64	244	38	48	80	
882	183*	81	71	329	45	49	96	
810	240	92	79	408	50	52	112	

[‡] All configurations are matched to produce same amount of neuronal membrane depolarization for membrane time constant of $\tau_m = 150 \mu\text{s}$.

[‡] total energy storage capacitance $C = C_1 + C_2$.

* approximate Magstim 200 configuration.